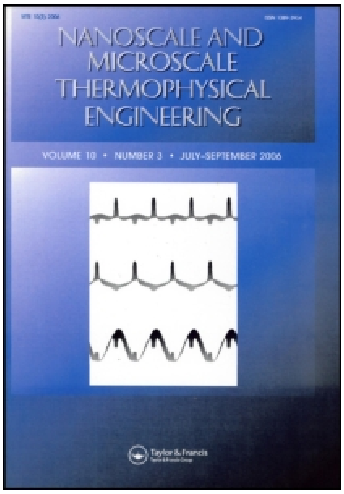

Nanoscale and Microscale Thermophysical Engineering
Publication details, including instructions for authors and subscription information:
http://www.informaworld.com/smpp/title~content=t713774103

The Kapitza Resistance Across Grain Boundary by Molecular Dynamics Simulation

Qiheng Tang [a]; Yugui Yao [b]
[a] LNM, State Key Laboratory of Nonlinear Mechanics, Institute of Mechanics, Chinese Academy of Sciences, Beijing, China [b] Institute of Physics, Chinese Academy of Sciences, Beijing, China

Online Publication Date: 01 December 2006

To cite this Article Tang, Qiheng and Yao, Yugui(2006)'The Kapitza Resistance Across Grain Boundary by Molecular Dynamics Simulation',Nanoscale and Microscale Thermophysical Engineering,10:4,387 — 398

To link to this Article: DOI: 10.1080/15567260601009239

URL: http://dx.doi.org/10.1080/15567260601009239

Nanoscale and Microscale Thermophysical Engineering, 10: 387–398, 2006

ISSN: 1556-7265 print / 1556-7273 online
DOI: 10.1080/15567260601009239

THE KAPITZA RESISTANCE ACROSS GRAIN BOUNDARY BY MOLECULAR DYNAMICS SIMULATION

Qiheng Tang
LNM, State Key Laboratory of Nonlinear Mechanics, Institute of Mechanics, Chinese Academy of Sciences, Beijing, China

Yugui Yao
Institute of Physics, Chinese Academy of Sciences, Beijing, China

Nonequilibrium molecular dynamics (NEMD) simulations are performed to calculate thermal boundary resistance that arises from heat flow across Si grain boundary. The environment-dependent interatomic potential (EDIP) on crystal silicon is adopted as a model system. The issues are related to nonlinear response, local thermal equilibrium, and statistical averaging. The tilt grain boundaries Σ5 and Σ13 are simulated, and the values of thermal boundary resistance by nonequilibrium molecular dynamics are compared with those by Maiti et al. (*Solid State Communications*, vol. 102, 1997). Using the disperse relation of EDIP potential, an average transmission coefficient of thermal conductivity across boundary is calculated.

KEY WORDS: the Kapitza resistance, grain boundaries, nonequilibrium molecular dynamics, phonons, thermal conduction

INTRODUCTION

With the dimension of electronic and mechanical devices approaching the nanometer scale, a demand for greater scientific understanding of thermal transport in nanoscale devices and individual nanostructures has been created. Some experimental and theoretical studies have been done to predict or measure thermal conductivity of nanowire, thin films, and periodic film structures [1–6]. Although current experimental techniques can study heat transfer at small scales, the spatial resolution is larger than 100 *nm* [7–9]. Moreover, interpretation of experimental results remain difficult because typically the different contribution of individual defects, such as impurities, grain boundaries, etc., cannot be deconvoluted clearly. Even for an individual grain boundary, Cahill et al. [10] pointed out that the interaction of phonons with a single interface still offers significant challenges to both experiments and theory/simulation.

There are currently two general theoretical frameworks for understanding the origin of the interfacial resistance for phonon-mediated thermal transport [11]. One is the

Received 15 November 2004; accepted 27 August 2006.

The research presented here was supported by the National Natural Science Foundation of China (grant nos. 10342001, 10372107, and 10404035) and Chinese Academy of Sciences (grant no. KJCX2-SW-L2), and supported by Supercomputing Center, CNIC, CAS.

Address correspondence to Qiheng Tang, LNM, State Key Laboratory of Nonlinear Mechanics, Institute of Mechanics, Chinese Academy of Sciences, No. 15 Beisihuanxi Road, Beijing, 100080, China. E-mail: qhtang@lnm.imech.ac.cn

acoustic mismatch model (AMM), in which the scattering of phonons at interface arises from the difference in the acoustic impedances of the materials on the two sides; the other is the diffuse mismatch model (DMM), which assumes that all incident phonons are randomly scattered by the interface. These two theories can successfully explain some heat transport of the mesoscale polycrystalline systems, but it can not take into account the atomistic structure of the interfaces from which the phonon scattering actually takes place.

There is a increasing demand to develop a method suitable for measuring thermal conductivity for the design of microelectronic devices. The molecular dynamics (MD) simulation method may provide a promising alternative technique both to calculate thermal conductivity and to understand defect mechanisms. MD now is extensively applied to calculate thermal properties because there is no need for an a priori understanding of heat transfer. Many MD simulations have been performed on the heat transfer of different structures, such as liquids [12], solids [13], solid–solid interface [14], and liquid–solid interface [15, 16].

Maiti et al. [14] used the direct method to perform the first simulations of thermal transport through symmetric tilt grain boundaries. The simulation shows a significant interfacial resistance. Schelling et al. [17] computed the Kapitza resistance of three twist grain boundaries in silicon by nonequilibrium molecular dynamics (NEMD) method and found that scattering depends strongly on the wavelength of the incident wave packet.

In the present article, NEMD is used to study heat transfer in the crystal silicon with the tilt grain boundary. First, we detail the simulation method, then we show the simulation results and report our conclusions.

COMPUTER SIMULATION

Interatomic Potential

Crystalline silicon is a semiconductor material extensively used in MEMS and integrated circuits. Heat conduction in semiconductor materials is dominated by phonon transport, and the contribution to heat conduction by the electrons is negligible. There are several categories of existing potential models for silicon, including the Tersoff type, the Stillinger-Weber (S-W) two- and three-body potentials [18], and others. The S-W potential has been used to simulate the thermal conductivity by several authors. Justo et al. [19] proposed the environment-dependent interatomic potential (EDIP), which can better describe the properties of silicon, such as the melting temperature and the thermal expansion coefficient. Therefore, EDIP potential is selected to simulate heat transfer in our work.

The EDIP potential can be expressed as

$$E_i = \sum_{j\neq i} V_2\left(r_{ij}, Z_i\right) + \sum_{j\neq i}\sum_{k\neq i,k>j} V_3\left(r_{ij}, r_{ik}, Z_i\right) \tag{1}$$

where $V_2(r_{ij}, Z_i)$ is an interaction between atoms i and j representing pairwise bonds, and $V_3(r_{ij}, r_{ik}, Z_i)$ is the interaction between atoms i, j, and k centered at atom i representing angular forces that can be defined by

$$V_2(r, Z) = A\left[\left(\frac{B}{r}\right)^p - p(Z)\right] exp\left(\frac{\sigma}{r-a}\right)$$

and

$$V_3(r_{ij}, T_{ik}, Z_i) = g(r_{ij})g(r_{ik})h(l_{ijk}, Z_i)$$

where $p(Z_i) = e^{-\beta Z_i^2}$, $l_{ijk} = \cos(\theta_{ijk}) = \overrightarrow{r}_{ij}, \overrightarrow{r}_{ik}/r_{ij}r_{ik}$, and Z_i is the effective coordination number, defined by

$$Z_i = \sum_{m \neq i} f(r_{im})$$

and $f(r_{im})$ is a cutoff function that measures the contribution of neighbor m to the atom i,

$$f(r_{im}) = \begin{cases} 1 & r_{im} \leq c \\ exp\left(\frac{\alpha}{1-x^{-3}}\right), & c \leq r_{im} \leq a; \\ 0 & r_{im} \geq a \end{cases}$$

where $x = (r - c)/(a - c)$, $g(r_{ij})$ is the radial function given by

$$g(r_{ij}) = exp\left(\frac{\gamma}{r_{ij} - a}\right)$$

and goes to zero smoothly at the cutoff distance a. The values of parameters of EDIP potential such as A, B, p, β, σ, a, c, λ, γ, Q_0, μ, and α are listed in *Table 1*.

Simulation Model

Since interfaces play a critical role in nanoscale thermal transport, an interface constitutes an interruption in the regular crystalline lattice on which phonons propagate. Many authors have suggested different simulation techniques to calculate the heat transfer. Some simulation results can be compared to those of experiments or theoretical analysis [20, 21] that activate one's interests of studies and application. The thermal gradient is applied along the heat flow direction by maintaining the two end sections at constant but different temperatures T_1 and T_2. Maiti et al. [14] calculated the Kapitza resistance of symmetric tilt grain boundary. In their simulation, the periodic boundary conditions are along the other two directions. Jund and Jullien [20] studied the thermal conductivity of vitreous silica, the techniques of the periodic boundary condition along x, y, z directions and the net kinetic energy increased/decreased by an amount $\Delta\epsilon$ in a thin slab are applied. Based on a similar NEMD method Schelling et al. [17] studied the Kapitza resistance of three twist rain boundaries. Using the same simulation technique as that of Jund and Jullien, the tilt grain boundaries $\Sigma 5$ and $\Sigma 13$ are simulated in the present article.

Table 1 Parameters in EDIP potential [19] for silicon

$A = 7.9821730\ (eV)$	$B = 1.5075463\ (eV)$	$\rho = 1.2085196$
$\alpha = 3.1213820\mathring{A}$	$c = 2.5609104\mathring{A}$	$\sigma = 0.5774108\mathring{A}$
$\lambda = 1.4531008eV$	$\gamma = 1.1247945\mathring{A}$	$\eta = 0.2523244$
$Q_0 = 312.1341346$	$\mu = 0.6966326$	$\beta = 0.0070975$
$\alpha = 3.1083847$		

Figure 1 is a schematic of a model system for heat conduction with a three-dimensional periodic simulation cell. A simulation system of parallelepiped cells with two symmetric tilt grain boundaries is selected in this study. The size of simulation cell is L_x, L_y, and L_z, respectively. Suppose that the heat transfer is along x direction, the size in x direction is larger than that in other directions. Figure 2 is atomistic configuration, it contains two grains misoriented with respect to each other by symmetric tilt rotation by some angle along [001] direction to generate two crystallographically boundaries, labeled GB 1 and GB 2. Their fully relaxed zero-temperature starting structures are obtained by static iterative energy minimization.

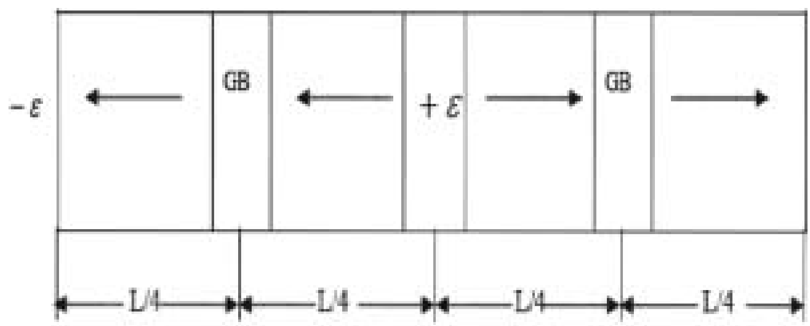

Figure 1. Schematic representation of three-dimensional periodic simulation cell. The simulation cell is parallelepiped with length L_x, L_y, and L_z. The heat flow is along the x direction. There are two symmetric tilt boundaries and a slab of thickness δ at $x = L_x/2$ into which energy $\Delta\epsilon$ is added; likewise, in the slab at $x = 0$, energy $\Delta\epsilon$ is removed.

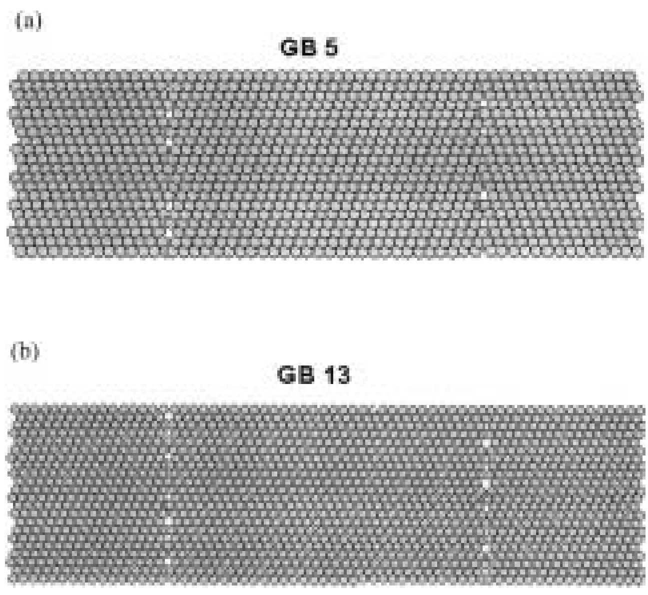

Figure 2. Atom configurations for simulation system. (a) (001) Σ 5 and (b) (001) Σ 13.

To calculate the temperature gradient, we divide the simulation cell into j slices along x direction. The temperature of particles in the thin slice is calculated at every iteration. The instantaneous temperature in each slice is calculated using the formula

$$(T_{MD})_j = \left\langle \sum_{i=1}^{N_j} m_i v_i^2 \right\rangle / 3N_j \kappa_B \tag{2}$$

where <> denotes statistical averaging overall of the simulation time, k_B is the Boltzmann constant, N_j is the atomic number in slice j, $(T_{MD})_j$ is the temperature in the *jth* slice, and m_i and v_i are the *ith* atom mass and velocity, respectively.

Simulations are of two stages. The first stage is the constant-temperature simulation, in which the temperature is maintained at constant value using weak coupling scheme [22] with a coupling time of 200,000 MD steps. $\Delta t = 0.539 \times 10^{-15} S$. The second stage is a constant-energy one. After equilibrium, a heat flux is imposed on the system along x direction. A small amount of kinetic energy $\Delta\epsilon$ is added in a thin slab centered at $x = L_x/2$ and removed from a slab of the same thickness centered at $x = 0$. Our simulations display that the distance between source and sink should be $L_x/2$ because of periodic boundary conditions. Each particle velocity in the source and sink regious is scaled by the same factor α, which is derived from an amount of net kinetic energy $\Delta\epsilon$ increased or decreased. To avoid an artificial drift of the kinetic energy, conservation of the total momentum in the source/sink slices is required. The velocity-rescaled arithmetic of Jund and Jullien [20] is used here.
By imposing the heat transfer in this manner a constant heat flux J_x can be calculated [23]

$$J_x = \Delta\epsilon / \left(2 L_y L_z \Delta t\right) \tag{3}$$

The temperature is calculated by Eq. (2) and temperature gradient is obtained. The relation between the current J_x and the temperature discontinuity at the interface ΔT is given as [17]

$$J_x = \sigma_\kappa \Delta T \tag{4}$$

where σ_K is known as the Kapitza conductance. The Kapitza resistance $R_\kappa = \frac{1}{\sigma_\kappa}$ is a measure of the resistance of an interface to the transport of heat through it.

RESULTS AND DISCUSSION

The resulting temperature profiles are shown in Figure 3. The system dimensions are 340 Å × 12.15 Å × 10.86 Å for (001)Σ5 boundary, and the length $L_x = 340$ Å is divided into 32 slices. The size of each slice is 10.625 Å × 12.15 Å × 10.86 Å. The total number of atoms is 2224, about 69 atoms per slice. Similarly, 443 Å × 13.84 Å × 10.86 Å for (001)Σ13, and the length $L_x = 443$ Å is divided into 40 slices for (001)Σ13 boundary. The total number of atoms is 3316, about 83 atoms per slice. The equilibrium temperature is 500 K.

According to the analysis of Maiti et al. [14], if there are more than 30 atoms in a slice, these would correspond to 3000 phonon scattering events in 1 *ns*, and the local thermal equilibrium can be obtained in the slice. A test of double slice number for

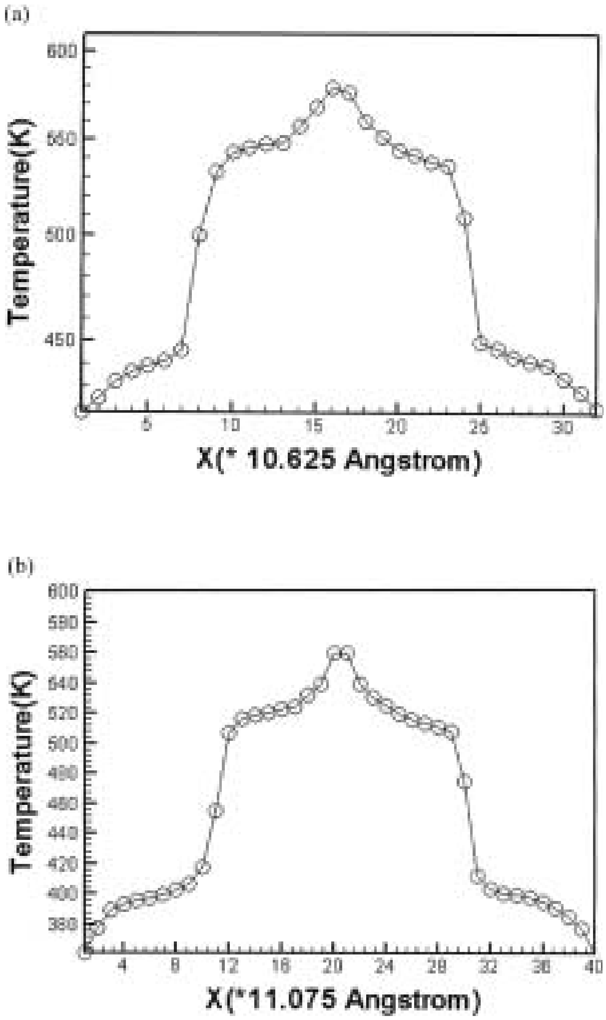

Figure 3. Typical temperature profiles. (a) 340 Å × 12.15 Å × 10.86 Å for (001) Σ 5 boundary; (b) 443 Å × 13.844 Å × 10.86 Å for (001) Σ 13. A nonlinear temperature profile observed near the regions of the source and sink.

(001)Σ13 is carried out, 80 slices are obtained, about 42 atoms per slice, temperature discontinuity will change a little, less than that of about 6%.

A nonlinear temperature profile is observed near regions of the heat source or heat sink, which has been attributed by the strong phonon scattering [20, 22]. The data of Figure 4 come from that of Figure 3. From Figure 4(a) and (b) temperature discontinuity 86 K and 84 K are calculated, respectively, and the average temperature $\Delta T = 85$ K. A suitable $\Delta\epsilon$ is taken as 1.2% of $\kappa_B T$, the energy increment $\Delta\epsilon = 0.000517eV$ is adopted in our simulations, and the heat flux $J_x = 58.22 \times 10^9$ (J/m^2s) and the thermal conductivity of about 0.685 (GW/m^2K) are obtained from Eqs. (6) and (7) for (001)Σ5 boundary. Similarly, for (001)Σ13 boundary, from Figures

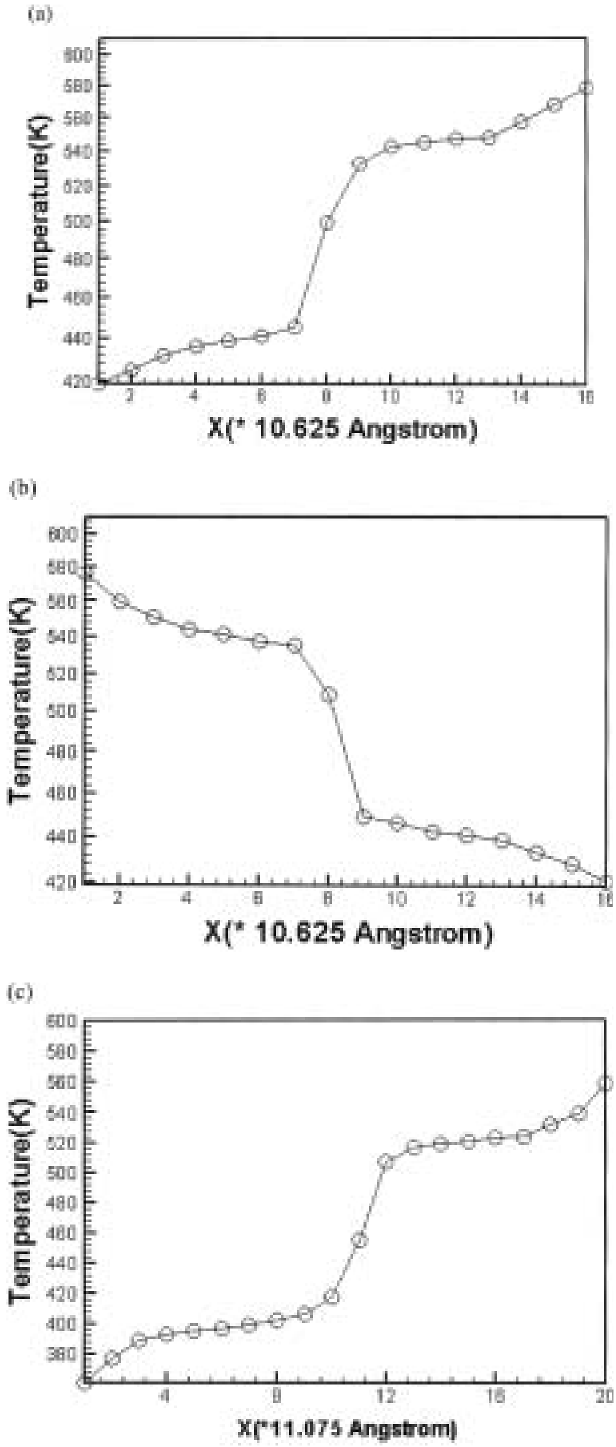

Figure 4. (a), (b) Typical temperature profiles for Σ 5 boundary; (c), (d) for Σ 13 boundary.

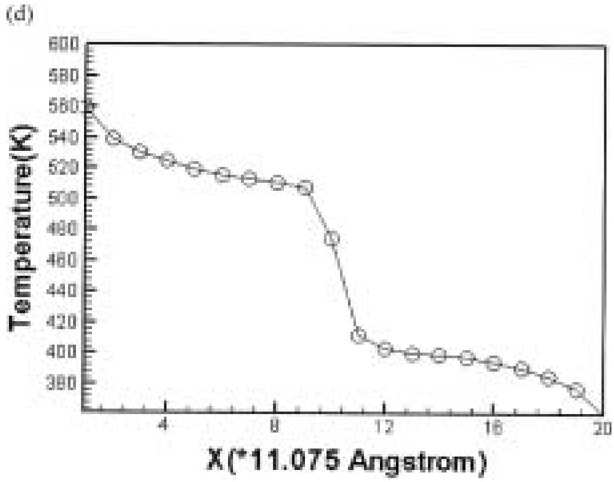

Figure 4. Continued.

4(c) and (d) temperature discontinuities of 90 K and 94 K are calculated, and the average temperature $\Delta T = 92$ K for (001)Σ13 boundary, $J_x = 51.11 \times 10^9$ (J/m^2s) and the thermal conductivity of about 0.562 (GW/m^2K).

It should be noted that the slice j temperature $(T_{MD})_j$ is obtained from Eq. (2), which is commonly used in MD simulation; however, it is a classical formula valid only at very high temperature $(T \gg T_{Debye})$, where $T_{Debye} = 645$ K is Debye temperature for silicon. In case the system average temperature ($T = 500$ K) is lower than the Debye temperature, it is necessary to apply a quantum correction. Because the system energy from classical statistics should equal to that from the quantum description,

$$3N_j k_B (T_{MD})_j = \int_0^{\omega_D} D_j(\omega) n_j(\omega, T) \hbar\omega d\omega \tag{5}$$

in which $D_j(\omega)$ is the density of states, $n_j(\omega, T)$ is the phonon occupation number, ω is the phonon frequency, and $\hbar$ the Planck's constant. From Eq. (4), we deduce the real system temperature T appearing in the function $n(\omega, T)$. Since the temperature gradient in the Fourier law must also be corrected, the thermal conductivity κ should be rescaled by the $\partial T_{MD}/\partial T$ factor obtained from Eq. (4). When the system temperature is 500 K, the correction coefficient $\partial T_{MD}/\partial T$ is nearly 1. The result given by Volz and Chen [24] shows that the influence of quantum correction on the thermal conductivity is not significant, and our calculations reach the same conclusion.

Figure 5 shows the evolution of time-averaged temperature for slice $j = 8.15$ nm, $j = 19$ nm, $j = 29.9$ nm, and $j = 40.73$ nm. Initially the system is in the unstable states, and temperature varies significantly for the first 300,000 MD steps, about 0.17 ns. The system reaches steady state at time greater than 1,000,000 MD steps, about 0.54 ns. This result indicates that 1.08 ns simulation time is a long enough to obtain time-averaged temperature profiles. It means that the local thermal equilibrium is reached within every slice region at 1 ns.

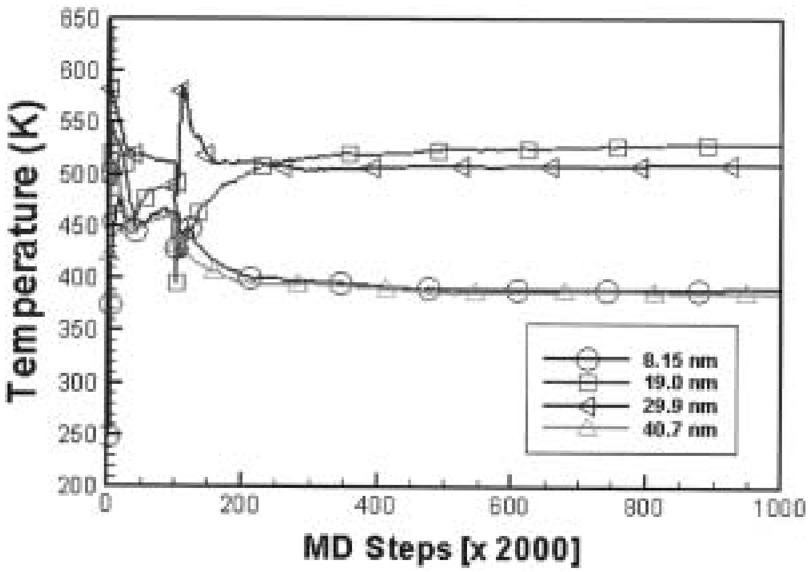

Figure 5. Time evolution of temperature for slices at 8.15 *nm*, 19 *nm*, 29.9 *nm*, and 40.7 *nm*, respectively.

By applying for a lattice dynamical model, we may analyze the Kapitza conductance theoretically. The Kapitza conductance can be expressed as the temperature derivative of the phonon heat current density across the interface [14]

$$\sigma_K = \sum_{\lambda} \int_{v_x>0} \frac{d^3q}{(2\pi)^3} \hbar\omega(\lambda, q) v_x(\lambda, q) \frac{\partial n(T)}{\partial T} t(\lambda, q) \tag{6}$$

where $t(\lambda,q)$ is the transmission coefficient of phonon, and v_x is the phonon group velocity normal to the boundary. The integration is over the entire Brillouin zone.

Calculating $t(\lambda,q)$ from phonon-matching equations is not straightforward for the case of a grain boundary. Once σ_K values are obtained from MD simulation, one can estimate an average transmission coefficient

$$< t >= \sigma_K / \sigma_K^{\max} \tag{7}$$

Taking $t(\lambda, q) = 1, \sigma\frac{\max}{K}$ is obtained from Eq. (6). The phonon dispersion relation of EDIP potential is used in Eq. (6). Applying for dynamical matrix of EDIP potential, we can obtain the phonon dispersion relation. The curves of frequency ω and group velocity ν versus wave vector are plotted in Figure 6 and Figure 7.

$\sigma\frac{\max}{K} = 1.2(GW/m^2K)$ is obtained from Eq. (6). So the average transmission coefficient $< t > = 0.57$ and 0.463 for (001) Σ5 and (001) Σ13 from Eq. (7), respectively. It means that the different atomic structure of interface may be with different thermal resistance for the same materials. By applying S-W potential, Maiti et al. [14] get $< t > = 0.65$ and 0.57. There is a little difference between our result and that of Maiti et al. The difference may be attributed to applying the different potentials and is within 12.3 and 18.77%, respectively, which is also within the range of the usual estimated calculating error value from about 10 to 20% [10].

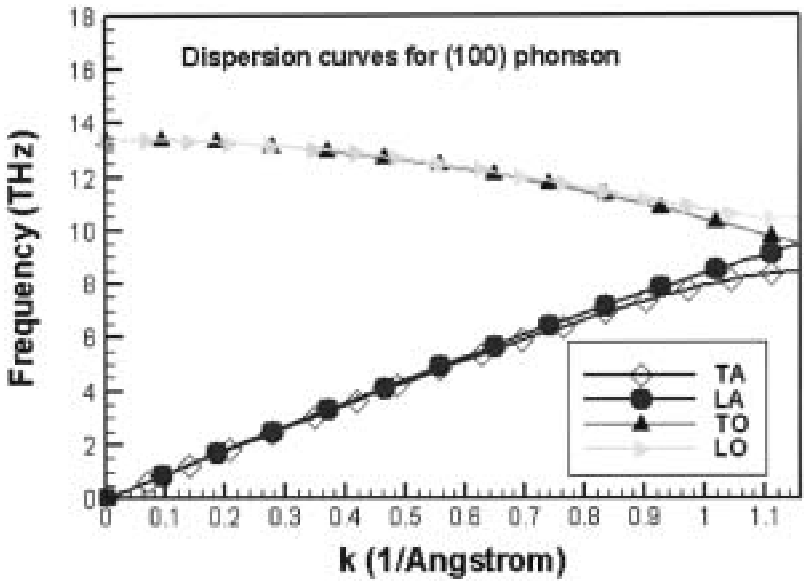

Figure 6. Dispersion relation of silicon for EDIP potential in (100) direction.

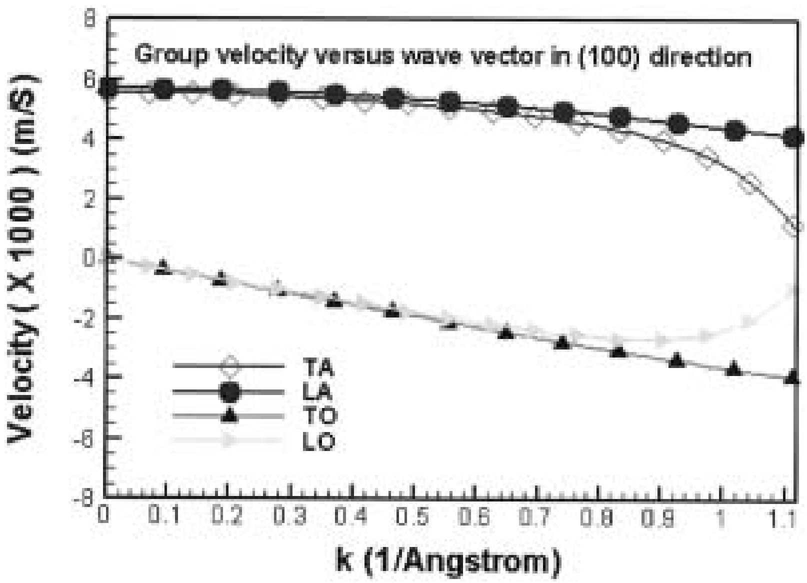

Figure 7. The curve of group velocity versus wave sector in (100) direction.

CONCLUSION

The NEMD with periodic boundary conditions is performed to determine the Kapitza conductance and Kapitza resistance for symmetric tilt grain boundaries (001) $\Sigma5$ and (001) $\Sigma13$. An obvious thermal boundary resistance is observed by simulation, and theoretic analysis show that about 57% phonon across grain boundary. The different grain boundaries are with different Kapitza conductance; the similar conclusion can be deduced by Maiti et al.'s [14] simulation.

REFERENCES

1. A.D. McConnell, S. Uma, and K.E. Goodson, Thermal Conductivity of Doped Polysilicon Layers, *Journal of Microelectromechanical Systems*, vol. 10, no. 3, pp. 360–369, 2001.
2. D.G. Cahill, K. Goodson, and A. Majumdar, Thermometry and Thermal Transport in Micro/Nanoscale Solid State Devices, *Journal of Heat Transfer*, vol. 124, pp. 223–241, 2002.
3. B. Li, L. Pottier, J.P. Roger, D. Fournier, K. Watari, and K. Hirao, Measuring the Anisotropic Thermal Diffusivity of Silicon Nitride Grains by Thermoreflectance Microsocopy, *Journal of the European Ceramic Society*, vol. 19, pp. 1631, 1999.
4. X. Wang, H. Hu, and X. Xu, Photo-Acoustic Measurement of Thermal Conductivity of Thin Films and Bulk Materials, *Journal of Heat Transfer*, vol. 123, pp. 138–144, 2001.
5. V.V. Kulish, J.L. Lage, P.L. Komorov, and P.E. Raad, A Fractional-Diffusion Theory for Calculating Thermal Properties of Thin Films from Surface Transient Thermoreflectance Measurements, *Journal of Heat Transfer*, vol. 123, pp. 1133–1138, 2001.
6. S. Mazumder and A. Majumdar, Monte Carlo Study of Phonon Transport in Solid Thin Films Including Dispersion and Polarization, *Journal of Heat Transfer*, vol. 123, pp. 749–759, 2001.
7. M. Asheghi, M.N. Touzelbaev, K.E. Goodson, Y.K. Leung, and S.S. Wong, Temperature-Dependent Thermal Conductivity of Single-Crystal Silicon Layers in SOI Substrates, *ASME Journal of Heat Transfer*, vol. 120, pp. 30–36, 1998.
8. Y.S. Ju and K.E. Goodson, Phonon-Scattering in Silicon Films with Thickness of Order 100 nm, *Applied Physics Letters*, vol. 74, pp. 3005–3007, 1999.
9. A. Asheghi, Y.K. Leung, S.S. Wong, and K.E. Goodson, Phonon-Boundary Scattering in Thin Silicon Layers, *Applied Physics Letters*, vol. 71, pp. 1798–1800, 1997.
10. D.G. Cahill, W.K. Ford, K.E. Goodson, G.D. Mahan, A. Majumdar, H.J. Maris, R. Merlin, and S.R. Phillpot, Nanoscale Thermal Transport, *Journal of Applied Physics*, vol. 93, pp. 793, 2003.
11. E.T. Swartz and R.O. Pohl, Thermal Boundary Resistance, *Reviews of Modern Physics*, vol. 61, no. 3, pp. 605–668, 1989.
12. W.T. Ashurst and W.G. Hoover, Dense-Fluid Shear Viscosity via Nonequilibrium Molecular Dynamics, *Physical Review A*, vol. 11, pp. 658–678, 1975.
13. M.P. Floian, A Simple Nonequilibrium Molecular Dynamics Method for Calculating the Thermal Conductivity, *Journal of Chemistry and Physics*, vol. 106, pp. 6082–6085, 1997.
14. A. Maiti, G.D. Mahan, and S.T. Pantelides, Dynamical Simulations of Nonequilibrium Processes — Heat Flow and the Kapitza Resistance and across Grain Boundaries, *Solid State Communications*, vol. 102, pp. 517–517, 1997.
15. J.L. Barrat and F. Chiaruttint, Kapitza Resistance at the Liquid-Solid Interface, *Molecular Physics*, vol. 101, pp. 1605–1610, 2003.
16. J.M. Kincaid, X. Li, and B. Hafskjold, Nonequilibrium Molecular Dynamics Calculation of the Thermal Diffusion Factor, *Fluid Phase Equilibria*, vol. 76, pp. 113–121, 1992.
17. P.K. Schelling, S.R. Phillpot, and P. Keblinski, Kapitza Conductance and Phonon Scattering at Grain Boundaries by Simulation, *Journal of Applied Physics*, vol. 95, no. 11, pp. 6082–6091, 2004.
18. F.H. Stillinger and T.A. Weber, Computer Simulation of Local Order in Condensed Phases of Silicon, *Physical Review B*, vol. 31, pp. 5262–5271, 1985.
19. J.F. Justo, V.V. Bulatov, and S. Yip, Interatomic Potential for Silicon Defects and Disordered Phases, *Physical Review B*, vol. 58, pp. 2539–2550, 1998.

20. P. Jund and R. Jullien, Molecular Dynamics Calculation of the Thermal Conductivity of Vitreous Silica, *Physical Review B*, vol. 59, pp. 13707–13711, 1999.
21. G. Ciccotti, G. Jacucci, and I.R. McDonald. Thought-Experiments by Molecular Dynamics, *Journal of Statistical Physics*, vol. 21, p. 22, 1979.
22. W.G. Hoover, Nonequilibrium Molecular Dynamics, *Annual Review Physical of Chemistry*, vol. 34, pp. 103–127, 1983.
23. P.K. Schelling, S.R. Phillpot, and P. Keblinski, Comparison of Atomic-Level Simulation Method for Computing Thermal Conductivity, *Physical Review B*, vol. 65, pp. 144306-1–144306-12, 2002.
24. S.G. Volz, and G. Chen, Molecular-Dynamics Simulation of Thermal Conductivity of Silicon Crystals, *Physical Review B*, vol. 61, pp. 2651–2656, 2002.